Journal of Power Sources 222 (2013) 344–350

Contents lists available at SciVerse ScienceDirect

Journal of Power Sources

journal homepage: www.elsevier.com/locate/jpowsour

Photoelectrochemical biofuel cells based on H_2-mesoporphyrin IX or Zn-mesoporphyrin IX sensitizer on titanium dioxide film electrode

Jing Yang [a,b], Ligang Feng [a], Fengzhan Si [a], Yuwei Zhang [a], Changpeng Liu [a], Wei Xing [a,*], Kunqi Wang [c,**]

[a] State Key Laboratory of Electroanalytical Chemistry, Changchun Institute of Applied Chemistry, Laboratory of Advanced Power Sources, Graduate School of the Chinese Academy of Sciences, 5625 Renmin Street, Changchun 130022, PR China
[b] School of Pharmaceutical Sciences, Changchun University of Chinese Medicine, 1035 Boshuo Road, Changchun 130117, PR China
[c] School of Science, Changchun Institute of Technology, 395 Kuanping Road, Changchun 130021, PR China

HIGHLIGHTS

- A new two-compartment photoelectrochemical biofuel cell is fabricated.
- This cell is based on H_2-mesoporphyrin IX or Zn-mesoporphyrin IX sensitizer.
- H_2-mesoporphyrin IX shows a better performance than Zn-mesoporphyrin IX.

ARTICLE INFO

Article history:
Received 30 May 2012
Received in revised form
20 August 2012
Accepted 22 August 2012
Available online 30 August 2012

Keywords:
Photoelectrochemical biofuel cell
Sensitizer
Porphyrin
Oxidation–reduction mechanism
Titanium dioxide film electrode

ABSTRACT

H_2-mesoporphyrin IX and Zn-mesoporphyrin IX have been investigated as sensitizers for the titanium dioxide (TiO_2) film electrode to construct a new two-compartment photoelectrochemical biofuel cell (PEBFC). The PEBFC can convert the light and chemical energy to electricity by consuming photons and oxidizing glucose. The two sensitizers are similar with two carboxyl anchoring groups, except that the central hydrogen atoms in the H_2-mesoporphyrin IX are replaced by zinc. To determine how cell performance is affected by the sensitizer, we analyze the photochemical and photoelectrochemical properties of the two sensitizers by physical characterization and photoelectrochemical experiments. The UV–Vis absorption spectra and X-ray photoelectron spectra (XPS) indicate that the interactions between the sensitizer and TiO_2 decrease in the order of H_2-mesoporphyrin IX > Zn-mesoporphyrin IX. The interactions are also determined by Fourier transform infrared (FTIR) spectra which indicate that the two sensitizers are adsorbed on the TiO_2 film through the carboxyl groups. The photovoltaic characteristics show the Zn-mesoporphyrin IX is less effective in comparison with the H_2-mesoporphyrin IX, since the Zn-mesoporphyrin IX enhances the back electron-transfer process, producing lower IPCE and current. These results reveal that the H_2-mesoporphyrin IX is a more efficient sensitizer compared with the Zn-mesoporphyrin IX for the PEBFC.

1. Introduction

The conversion of solar to electric energy is a promising method of meeting the global demand for energy in the long term, since sunlight is inexhaustible, low-cost, environmentally clean and widely distributed geographically. Recently, a new type of photoelectrochemical biofuel cell (PEBFC) has been extensively reported, and it can convert the light and chemical energy to electric energy by combining a dye-sensitized solar cell (DSSC) with an enzyme-catalyzed biofuel cell (BFC) [1–8] (Fig. 1). This new cell uses the same dye-sensitized photoanode and cathode, but the electrolyte is different from that of the DSSC. Porphyrin has been extensively studied as a sensitizer due to the delocalized macrocyclic structure and very strong absorption in the 400–450 nm region (Soret band) as well as absorption in the 500–700 nm region (Q-bands) [9–14]. In addition, the rate of charge recombination between conduction band electron and oxidized porphyrin is in the range of several milliseconds; the time is sufficient to permit the regeneration of the ground state of the porphyrin at the electrode [9–14]. The porphyrin with one [1–6] or four carboxyl anchoring groups [15] is used as a sensitizer for the PEBFC and it is expected that the number of carboxyl anchoring group may influence the photosensitization behavior of the sensitizer on the surface of the titanium dioxide

* Corresponding author. Tel.: +86 431 85262223; fax: +86 431 85685653.
** Corresponding author.
E-mail addresses: xingwei@ciac.jl.cn (W. Xing), wkq@ciac.jl.cn (K. Wang).

0378-7753/$ – see front matter
http://dx.doi.org/10.1016/j.jpowsour.2012.08.062

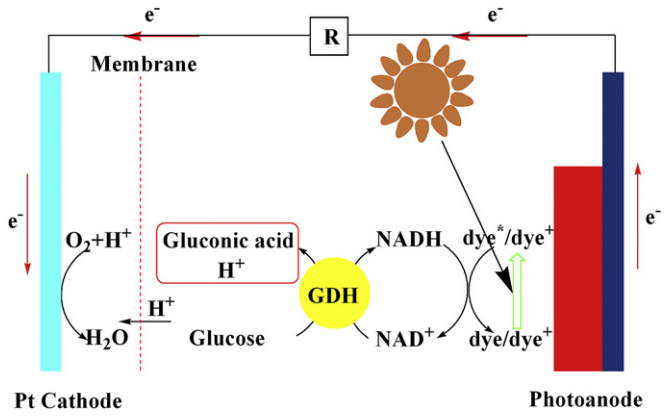

Fig. 1. Schematic diagram of the oxidation–reduction mechanism for the PEBFC.

(TiO_2) film electrode. The adsorption state of the sensitizer on the surface of the TiO_2 significantly influences the performance of the PEBFC. In this paper, a H_2-mesoporphyrin IX with two carboxyl anchoring groups (Fig. 2a) and its derivative Zn-mesoporphyrin IX (Fig. 2b) were used as sensitizers for TiO_2 film electrodes to fabricate PEBFCs. The central part of the Zn-mesoporphyrin IX is occupied by a zinc ion linked to a pyrrole ring. We characterized and compared the Fourier transform infrared (FTIR), X-ray photoelectron spectra (XPS) and UV–Vis absorption spectra of H_2-mesoporphyrin IX and Zn-mesoporphyrin IX in solution, in the solid state and adsorbed onto the TiO_2 electrode, and evaluated the photochemical and photoelectrochemical properties of the two PEBFCs. The properties were strongly influenced by the insertion of zinc ion in the porphyrin sensitizer and the interaction between the sensitizer and TiO_2 film electrode. Compared with the PEBFC based on the photosensitization of Zn-mesoporphyrin IX, the PEBFC with H_2-mesoporphyrin IX sensitizer demonstrates much higher incident photon-to-collected electron conversion efficiency (IPCE) and better photovoltaic performance. The result may be due to the fact that the oxidized metallized porphyrin enhances the back electron-transfer process, producing lower photocurrent. Thus, the H_2-mesoporphyrin IX is a more attractive sensitizer which can improve the photoelectrochemical properties of the PEBFC compared with the Zn-mesoporphyrin IX.

2. Experimental

2.1. Materials

All solvents and reagents, unless otherwise stated, were of analytical grade and used without further purification. H_2-mesoporphyrin IX and Zn-mesoporphyrin IX were purchased from Aladdin Company. β-nicotinamide adenine dinucleotide reduced form disodium salt (β-NADH) was obtained from Sigma–Aldrich Company. Perfluorinated sulfonic acid proton-exchange membrane Nafion 117 (thickness: 80 μm, exchange capacity: 1.0 ± 0.02 mM g^{-1}) was obtained from Shandong Dongyue Shenzhou New Material Co, Shandong China. The trishydroxylaminomethane (Tris) was purchased from J&K Chemical Ltd. The glucose dehydrogenase (GDH) was purchased from Toyobo Co., Ltd. The enzyme activity was assayed following a protocol provided by the manufacturer. β-D-glucose, *N*,*N*-dimethyl formamide (DMF) and potassium chloride (KCl) were purchased from Beijing Chemical Company (Beijing, China). 3α,7α-dihyroxy-5β-cholic acid (cheno) was purchased from Fluka. One unit of GDH activity is defined as the amount of enzyme per minute that reduced 1.0 mmol NAD^+ to NADH by glucose.

2.2. Preparation of TiO_2 film electrode

Firstly, a 7-μm-thick transparent layer of TiO_2 particles was deposited via the screen-printing protocol onto a precleaned fluorine-doped tin oxide (FTO) conductive glass (Nippon Sheet Glass, Solar, 4 mm thick), and subsequently the second layer of scattering TiO_2 particles with 5-μm thick was coated on the first layer. The detailed preparation procedures of TiO_2 nanoparticles, pastes for screen printing and double-layer circular TiO_2 film have been reported in the previous literature [16].

2.3. Preparation of platinum-coated fluorine-doped tin oxide electrode

The platinum-coated FTO electrode was prepared by thermal decomposition of hydrogen hexachloplatinate hexahydrate. The detailed procedure was as follows: firstly, the hydrogen hexachloplatinate hexahydrate in 2-propanol solution (2 mg Pt mL^{-1} solution) was coated on the FTO glass plate at room temperature.

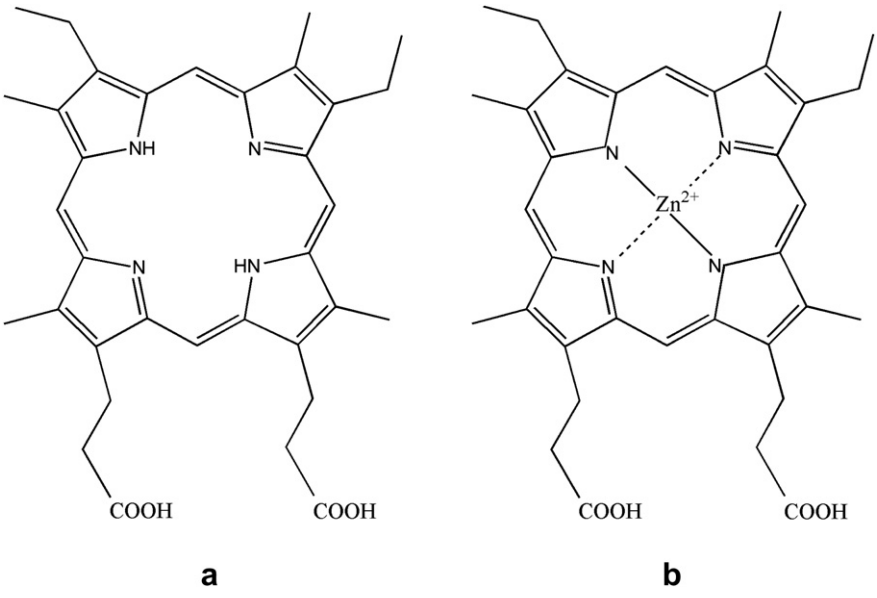

Fig. 2. Molecular structures of (a) H_2-mesoporphyrin IX and (b) Zn-mesoporphyrin IX.

Secondly, the FTO glass plate was annealed at 400 °C for 10 min, and then cooled to room temperature.

2.4. Fabrications of photoelectrochemical biofuel cell

The TiO_2-coated FTO conductive glass electrode was heated for 30 min at 550 °C, and then cooled to 80 °C. The above electrode was dipped for 5 h in ethanol solution containing 5×10^{-5} M of H_2-mesoporphyrin IX and 5×10^{-4} M of coadsorbate cheno or in DMF solution containing 5×10^{-5} M of Zn-mesoporphyrin IX and 5×10^{-4} M of coadsorbate cheno. The apparent surface area of the prepared photoanode FTO/TiO_2/H_2-mesoporphyrin IX (or Zn-mesoporphyrin IX) was 0.228 cm^2.

Three grooves were machined on the surface of the high density polyethylene block, and each groove size was 16 mm × 10 mm × 3 mm. A Nafion 117 proton-exchange membrane was sandwiched in the middle groove between the two grooves by two high density polyethylene rings. The dye-sensitized photoanode and the cathode were put into the two grooves to fabricate a two-compartment PEBFC. The anodic compartment was filled with the solution containing 4 mM NADH, 0.1 M glucose, 0.015 units mL^{-1} GDH and 0.25 M Tris buffer at pH 8 which was adjusted with HCl; the buffer contained 0.1 M KCl as the supporting electrolyte. Nitrogen gas was purged into the anodic compartment to exclude oxygen. The cathodic compartment was filled with an oxygen-saturated solution containing 0.25 M Tris buffer and 0.1 M KCl as the supporting electrolyte at pH 8. The edge of the groove with the photoanode is open for harvesting light, and silicon gel is used to adhere the photoanode to the groove for preventing the leak of the electrolyte. It should be noted that the photoanode and cathode can not completely be submerged in electrolyte, so that both the electrodes can be wired to an external circuit.

2.5. UV–Vis, Fourier transform infrared and X-ray photoelectron spectroscopy measurements

Absorption spectra were performed on a UNICO WFZ UV-2802PC/PCS spectrometer. The Fourier transform infrared (FTIR) spectra were measured using a BRUKER Vertex 70 FTIR spectrometer. The TiO_2 film photoanodes sensitized by sensitizers were rinsed with ethanol or DMF, and then dried prior to measuring the spectra. X-ray photoelectron spectra (XPS) measurements were recorded by using a Kratos XSAM-800 spectrometer with Mg Kα radiator.

2.6. Photovoltaic characteristics

A Keithley 2400 source meter and a Zolix Omni-λ300 monochromator equipped with a 500 W xenon lamp were used for photocurrent action spectrum measurements with a wavelength sampling interval of 10 nm and a current sampling interval of 2 s under full computer control. A Hamamatsu S1337-1010BQ silicon diode used for IPCE measurements was calibrated at the National Institute of Metrology, China. A model LS1000-4S-AM1.5G-1000W solar simulator (Solar Light Co., Glenside, PA) was employed to give an irradiance of 100 mW cm^{-2}. The light intensity was tested with a PMA2144 pyranometer and a calibrated PMA 2100 dose control system. The current–voltage characteristics were measured with a Keithley 2602 source meter under full computer control. The measurements were fully automated using Labview 8.0 (USA).

All photoelectrochemical measurements are carried out immediately at room temperature after the cells are fabricated.

2.7. Electrochemical experiments

Electrochemical measurements were carried out with an EG&G model 273 potentiostat/galvanostat and a conventional three-compartment electrochemical cell. The current measurements contained a TiO_2 or TiO_2/H_2-mesoporphyrin IX coated FTO working electrode (area = 0.228 cm^2), a platinum wire counter electrode and a Hg/Hg_2Cl_2 (saturated KCl solution) reference electrode. The electrochemical cell was in a dark box in order to isolate the system from external light sources. The solution containing 0.13 mg mL^{-1} NADH, 0.1 M KCl and 0.25 M Tris buffer at pH 8 was prepared with Millipore water and deaerated with nitrogen gas.

3. Results and discussion

3.1. Characterization of the photoanode

3.1.1. UV–Vis absorption spectra of dye-sensitized TiO_2 film electrode

The UV–Vis absorption spectra of the sensitizer H_2-mesoporphyrin IX or Zn-mesoporphyrin IX in a solution and on a mesoporous TiO_2 film electrode were measured so as to have a preliminary evaluation on their light-harvesting capacity as shown in Fig. 3. In Fig. 3a, the UV–Vis absorption spectrum of the sensitizer H_2-mesoporphyrin IX in the ethanol and coadsorbate solution includes a Soret band at 415 nm and Q-bands at 498, 530, 561 and 602 nm, which are in good agreement with those previously reported for similar porphyrins [17–21]. The UV–Vis absorption spectrum of the sensitizer H_2-mesoporphyrin IX coated on the mesoporous TiO_2 film electrode in the Soret band is at 407 nm, which is slightly blue-shifted by 8 nm compared with that in the solution; the absorption peaks in the Q-band region are at 507, 533, 574 and 625 nm, which are slightly red-shifted by 9, 3, 13 and 23 nm, compared with those in the solution, respectively. The number of the peaks is three for Zn-mesoporphyrin IX in the

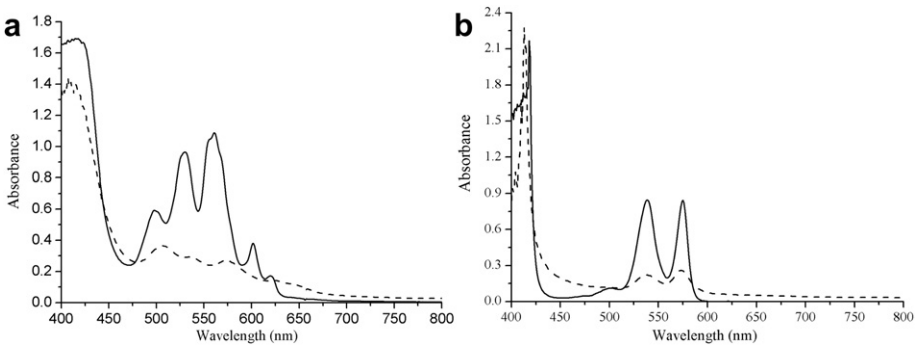

Fig. 3. (a) Absorption spectra of 5×10^{-5} M H_2-mesoporphyrin IX in ethanol solution containing 5×10^{-4} M 3α,7α-dihyroxy-5β-cholic acid (solid line) and H_2-mesoporphyrin IX coated on TiO_2 electrode (dashed line). (b) Absorption spectra of 5×10^{-5} M Zn-mesoporphyrin IX in DMF solution containing 5×10^{-4} M 3α,7α-dihyroxy-5β-cholic acid solution (solid line) and Zn-mesoporphyrin IX coated on TiO_2 electrode (dashed line).

visible region and the number of Q-bands is reduced compared with H_2-mesoporphyrin IX. The absorption spectrum of Zn-mesoporphyrin IX in DMF and coadsorbate solution (Fig. 3b, solid line) shows a strong peak at about 418 nm (Soret band) and only two smaller peaks at 539 and 575 nm (Q-bands). When Zn-mesoporphyrin IX was adsorbed on the TiO_2 film, an intense Soret band at 413 nm was observed (Fig. 3b, dotted line), which showed a slightly blue shift by 5 nm compared with the absorption peak of the sensitizer Zn-mesoporphyrin IX in the solution; the peaks at Q-bands were consistent with the corresponding spectra of Zn-mesoporphyrin IX in the solution. On the TiO_2 film electrode the shift of peak value is due to the electronic coupling between the π orbital of the sensitizer and the *d* orbital of TiO_2 resulted from the chemical linkage [22]. For the sensitizer Zn-mesoporphyrin IX, it is obvious that the value of the shift is smaller than that for H_2-mesoporphyrin IX. This means that the interaction between Zn-mesoporphyrin IX and the TiO_2 surface is weaker than that of H_2-mesoporphyrin IX and the TiO_2 surface owing to the insertion of zinc ion [20].

3.1.2. Feature of FTIR spectra

The above results of UV–Vis absorption spectra have proved that there is a substantial interaction between sensitizer and TiO_2 film, but the modes of the interaction are not yet clear. Thus, to investigate the coordination states of the sensitizers on the TiO_2 film surfaces, the FTIR spectra of the sensitizers in the solid state and the adsorption state on the TiO_2 film were measured. Fig. 4 shows the FTIR absorption spectra of sensitizers over the range of 500–4000 cm^{-1} at room temperature. Fig. 4a displays the FTIR spectra of TiO_2 film, H_2-mesoporphyrin IX sensitizer powder and the sensitizer coated on a TiO_2 film for comparison. The peaks of C=O bond in carboxyl group were observed at 1738 and 1527 cm^{-1} for the H_2-mesoporphyrin IX in the solid state. The FTIR spectrum of the sensitizer coated on the TiO_2 film clearly shows the peaks at 1638 and 1406 cm^{-1}; they correspond to the asymmetric and symmetric stretching vibration of the carboxyl groups, indicating that the carboxylic acid group is deprotonated and takes part in the adsorption of the sensitizer on the surface of TiO_2 film [22,23]. FTIR absorption spectrum of the pure Zn-mesoporphyrin IX in the solid state shows the intense peaks at 1707 and 1452 cm^{-1} as can be seen from Fig. 4b which are assigned to the asymmetric and symmetric stretching vibration of the carboxyl group. When Zn-mesoporphyrin IX was adsorbed on the TiO_2 film, two intensive peaks were observed at 1632 and 1419 cm^{-1}; the two peaks can be assigned to the asymmetric and symmetric stretching vibration of the carboxyl group. From the above FTIR data, it may be inferred that both H_2-mesoporphyrin IX and Zn-mesoporphyrin IX are anchored on the TiO_2 film surface through the carboxyl groups via a bidentate or a bridging chelation with TiO_2 surface rather than an ester type linkage with TiO_2 surface [24]. As shown in Fig. 4, there was no obvious peak in the 500–4000 cm^{-1} range for the surface of TiO_2 film.

3.1.3. Characterization of XPS spectra

It is known that XPS is a highly surface-selective technique, so XPS is used to distinguish the surface change of pure TiO_2 film before and after adsorption of H_2-mesoporphyrin IX or Zn-mesoporphyrin IX [25–28]. Under the same conditions, the XPS spectra of Ti (2p) and O (1s) for the TiO_2 film, the TiO_2 film coated with H_2-mesoporphyrin IX (H_2-mesoporphyrin IX/TiO_2) and the TiO_2 film coated with Zn-mesoporphyrin IX (Zn-mesoporphyrin IX/TiO_2) were compared in Fig. 5. Parameters of the XPS obtained from Fig. 5 for Ti ($2p_{3/2}$), Ti ($2p_{1/2}$) and O (1s) are listed in Table 1. Compared with the peaks of a blank TiO_2 electrode, for the Zn-mesoporphyrin IX/TiO_2, the peaks of Ti ($2p_{3/2}$) and Ti ($2p_{1/2}$) show a slight shift by 0.02 eV and 0.31 eV, respectively, while the shifts for the H_2-mesoporphyrin IX/TiO_2 are 0.08 and 0.36 eV, respectively (Fig. 5a). For the Zn-mesoporphyrin IX/TiO_2, the shift of the peak is smaller than that for the H_2-mesoporphyrin IX/TiO_2. In the O (1s), similar phenomena were also observed as shown in Fig. 5a and Table 1. These results indicate that the interaction between the sensitizer and TiO_2 decreases in the order of H_2-mesoporphyrin IX > Zn-mesoporphyrin IX, which is very consistent with the observed results from the UV–Vis spectra.

3.2. Oxidation–reduction mechanism of the photoelectrochemical biofuel cell

The oxidation–reduction mechanism of the two-compartment PEBFC is shown in Fig. 1. The PEBFC relies upon charge separation at a dye-sensitized TiO_2 semiconductor film photoanode. The dye is excited by visible photon, resulting in electron injection from the excited dye into the conduction band of TiO_2; these electrons are collected at the FTO conductive glass and passed to the cathode by an external circuit. The produced dye in oxidized state (dye^+) oxidizes the β-NADH to β-nicotinamide adenine dinucleotide (β-NAD^+) which can serve as an electron acceptor; β-D-glucose under the catalysis of GDH gives electrons to β-NAD^+ (Fig. 1). The mechanism shows that β-NADH is an important electron donor to the oxidized dye at the photoanode [1]. The photoanode is in the anodic compartment which is filled with an electrolyte of 4 mM NADH, 0.1 M glucose, 0.015 units mL^{-1} GDH, 0.25 M Tris and 0.1 M KCl at pH 8 (adjusted with HCl) [29]. The anodic compartment is

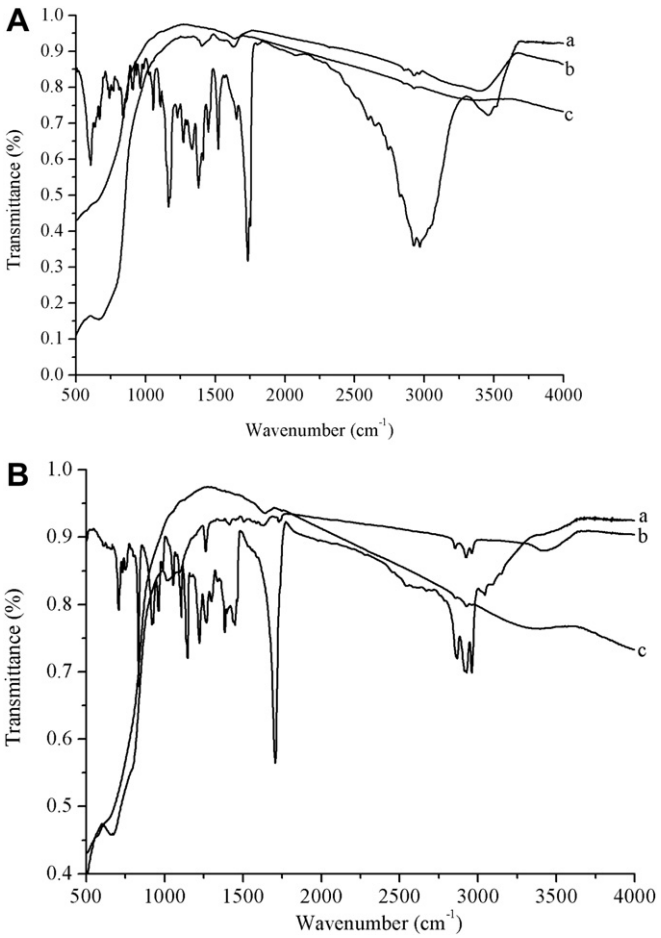

Fig. 4. (A) FTIR spectra of (a) H_2-mesoporphyrin IX sensitizer, (b) the sensitizer coated on a TiO_2 film and (c) TiO_2 film. (B) FTIR spectra of (a) Zn-mesoporphyrin IX sensitizer, (b) the sensitizer coated on a TiO_2 film and (c) TiO_2 film.

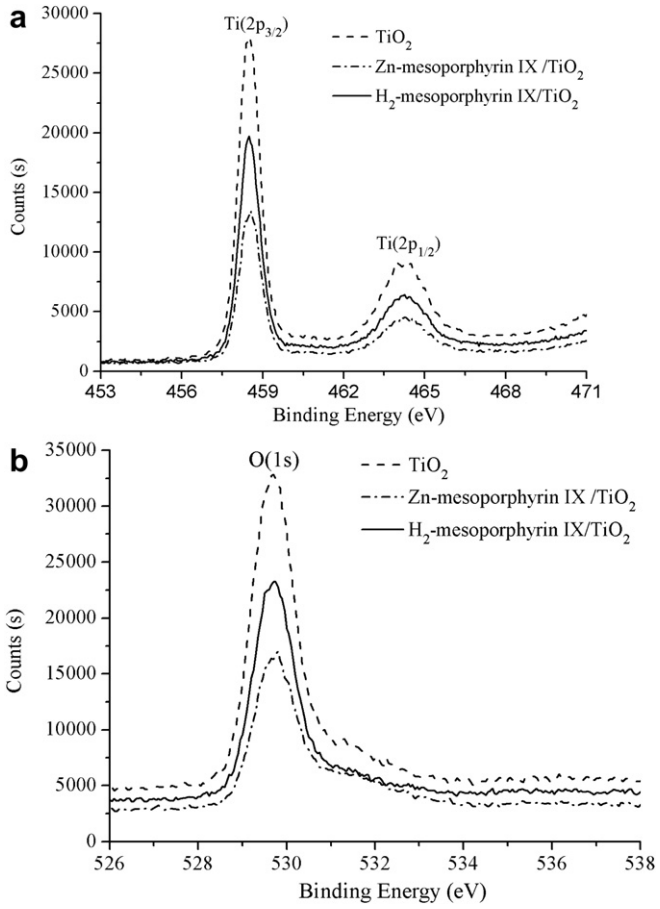

Fig. 5. XPS spectra of (a) Ti ($2p_{3/2}$), Ti ($2p_{1/2}$) and (b) O (1s) for TiO_2, H_2-mesoporphyrin IX/TiO_2 and Zn-mesoporphyrin IX/TiO_2.

separated from the cathodic compartment by the perfluorinated sulfonic acid proton-exchange membrane (Nafion 117). The hydrogen ion produced in the anodic compartment diffuses to the cathodic compartment through the Nafion 117 membrane. At the platinum-coated fluorine-doped tin oxide cathode, water is produced by the reaction of oxygen and hydrogen ion with the help of platinum catalyst.

3.3. Photocurrent action spectrum

To comparatively evaluate the performance of the two sensitizers, the photocurrent action spectra for PEBFCs with the TiO_2 films sensitized by H_2-mesoporphyrin IX or Zn-mesoporphyrin IX are shown in Fig. 6. The onset wavelengths of the IPCE spectra for the PEBFCs based on H_2-mesoporphyrin IX or Zn-mesoporphyrin IX sensitizer were less than 750 nm. The IPCEs of the two PEBFCs at some wavelength are much higher than those of the reported porphyrin with one carboxyl anchoring group [1–6] but less than that of the reported porphyrin with four carboxyl anchoring groups

Table 1
XPS of Ti ($2p_{3/2}$), Ti ($2p_{1/2}$) and O (1s) obtained from the curve fits of Fig. 5.

	Binding energy (eV)		
	Ti ($2p_{3/2}$)	Ti ($2p_{1/2}$)	O (1s)
TiO_2	458.47	463.91	529.68
H_2-mesoporphyrin IX/TiO_2	458.55	464.27	529.79
Zn-mesoporphyrin IX/TiO_2	458.49	464.22	529.76

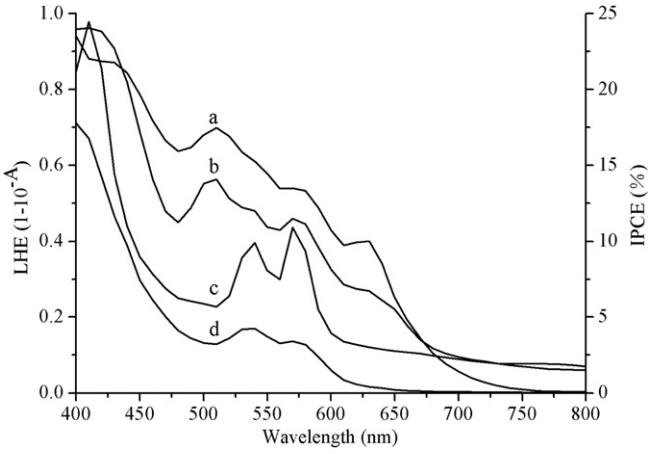

Fig. 6. Photocurrent action spectra and light-harvesting efficiencies of the photoelectrochemical biofuel cells with (a, b) H_2-mesoporphyrin IX or (c, d) Zn-mesoporphyrin IX sensitizer.

[15]. The result may be attributed to more effective electron injection and transfer to the TiO_2 semiconductor for the sensitizer with more carboxyl anchoring groups [20,30–32]. The result indicates that the IPCE increases with the increase of the carboxyl anchoring group of the sensitizer for the PEBFC. The absorption peaks in the photocurrent action spectra for the PEBFC with H_2-mesoporphyrin IX sensitizer are observed at 430, 510, 580 and 630 nm, and the corresponding IPCEs are ca. 22%, 17%, 13% and 10%, respectively (Fig. 6a). For the PEBFC with Zn-mesoporphyrin IX sensitizer, the corresponding IPCE values at 410, 540 and 578 nm are 17%, 4% and 3%, respectively, as shown in Fig. 6d. The maximum IPCE value for the PEBFC based on Zn-mesoporphyrin IX sensitizer was lower than that of the PEBFC with H_2-mesoporphyrin IX sensitizer due to the introduction of the zinc ion into the porphyrin. A possible reason for the lower IPCE in the Zn-mesoporphyrin IX is that the back electron-transfer process is higher [20,33]. The back electron-transfer process shows to be the major limiting factor in achieving high IPCE value [34–36].

The light-harvesting efficiency (LHE) at any particular wavelength is calculated by formulas $1-10^{-A}$, where A is the absorbance which may be estimated from a spectrum such as shown in Fig. 3. The LHE curves of TiO_2 film electrodes sensitized by H_2-mesoporphyrin IX or Zn-mesoporphyrin IX are also shown in Fig. 6. There are some similarities between the IPCE and LHE curves for every sensitizer. For example, at near 410, 510, 570 and 630 nm, photons can be trapped, and the photogenerated electrons can be injected into the external circuit of the PEBFC with H_2-mesoporphyrin IX sensitizer (Fig. 6b). For the PEBFC with Zn-mesoporphyrin IX sensitizer, the processes of optical trapping and electron injection occur at near 410, 540 and 570 nm (Fig. 6c). The shapes of IPCE and LHE curves for the PEBFCs with H_2-mesoporphyrin IX or Zn-mesoporphyrin IX dye are also close to those in the UV–Vis absorption spectra of sensitizers in solution and on TiO_2 film electrode, indicating that light absorbed by sensitizers is responsible for the photocurrent.

3.4. Current–voltage curve

The photoanodes with 0.228 cm^2 are illuminated with 100 mW cm^{-2}; the current–voltage curves obtained for the PEBFCs with H_2-mesoporphyrin IX or Zn-mesoporphyrin IX sensitizer are shown in Fig. 7. The performance characteristics of the PEBFCs are summarized in Table 2. As shown in Fig. 7 and Table 2, the photoelectrochemical characteristics for the two PEBFCs are quite

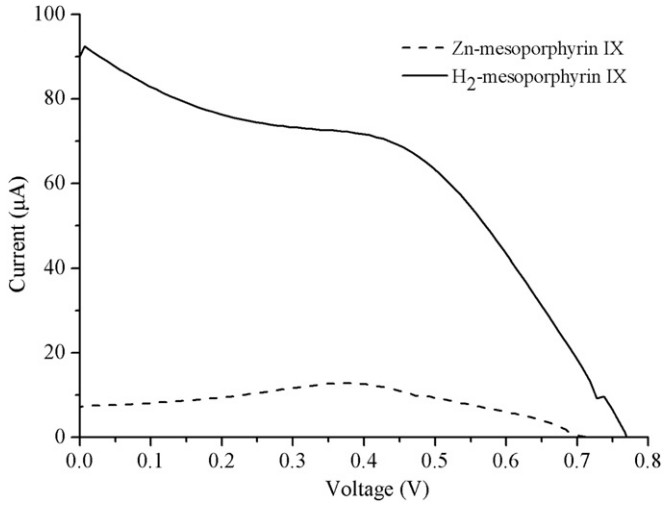

Fig. 7. Current–voltage characteristics for the PEBFCs with H_2-mesoporphyrin IX or Zn-mesoporphyrin IX as sensitizer under light intensity of 100 mW cm^{-2} condition.

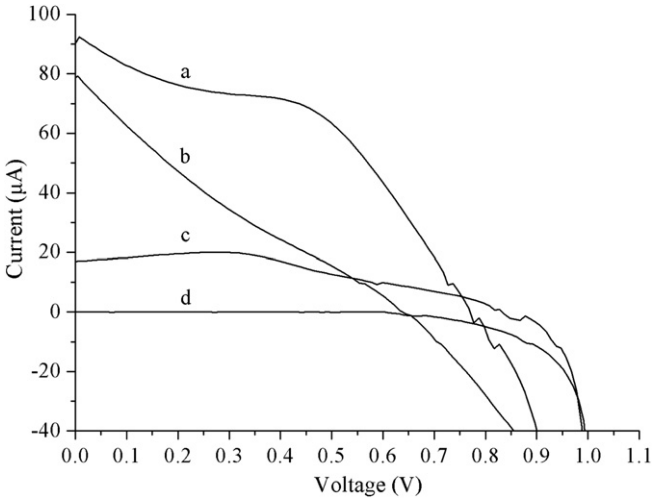

Fig. 8. Current–voltage characteristics for the PEBFCs in the presence (a) and absence of fuel glucose (c), in the absence of the sensitizer, GDH and NADH (b) and in the absence of the light (d).

different. The short-circuit current (I_{sc}), the open-circuit potential (V_{oc}), maximum power density (P_{max}) and fill factor (FF) of the PEBFC made from Zn-mesoporphyrin IX are 7 μA, 713 mV, 22 μW cm^{-2} and 0.99, respectively; this cell yields an overall energy conversion efficiency (η) of 0.022%. In contrast, the photovoltaic parameters, I_{sc}, V_{oc} P_{max}, FF and η, of the PEBFC with H_2-mesoporphyrin IX as a sensitizer are 90 μA, 767 mV, 139 μW cm^{-2}, 0.46 and 0.14%, respectively. Especially, the short-circuit current (I_{sc}), the open-circuit potential (V_{oc}), maximum power density (P_{max}) and overall energy conversion efficiency (η) for the PEBFC with the H_2-mesoporphyrin IX sensitizer are greater than those of the PEBFC with the Zn-mesoporphyrin IX sensitizer. The fact that the generation of photoelectrical effects for the Zn-mesoporphyrin IX is less effective than the H_2-mesoporphyrin IX may be explained by following process: because the metallized porphyrin can enhance the back process of electron-transfer, the metallized Zn-mesoporphyrin IX produces the lower photocurrent than H_2-mesoporphyrin IX [37]. However, according to the equation of fill factor (FF), $FF = P_{max}/I_{sc}V_{oc}$, the FF observed for the PEBFC with the H_2-mesoporphyrin IX is lower than the PEBFC with the Zn-mesoporphyrin IX, which may stem from the higher I_{sc} and V_{oc} for the PEBFC with H_2-mesoporphyrin IX sensitizer.

Several control experiments were done to reveal the feature of the PEBFC sensitized by H_2-mesoporphyrin IX dye, as shown in Fig. 8. Specifically, the current–voltage curve in the presence (Fig. 8a) and absence (Fig. 8c) of fuel glucose demonstrated that the glucose dramatically effected the current and voltage. In the absence of glucose the produced NAD^+ can not be reduced back to NADH by GDH during oxidation of glucose. And the amount of the available NADH is low, producing low current (I_{sc}=17 μA), which is very consistent with the oxidation–reduction mechanism of the PEBFC. However, in the absence of glucose (Fig. 8c) the PEBFC can operate at a high V_{oc} (0.82 V). In the absence of the sensitizer, GDH and NADH (Fig. 8b) the V_{oc} of the PEBFC is 0.63 V. The above results show that the anode potential in the PEBFC is limited by the sensitizer, fuel glucose and NADH. In the absence of light the current was negligible (Fig. 8d), and the control experiment confirmed that the light played an important role for the generation of current. The results of control experiments for the PEBFC with Zn-mesoporphyrin IX sensitizer were in consistency with those for the PEBFC with H_2-mesoporphyrin IX sensitizer.

In order to understand the electrochemical mechanisms occuring at the photoanode, half cell electrochemical measurements were carried out (Fig. 9). The current increased with increasing applied potential within a range of −0.2 to 1.0 V. The current for FTO/TiO_2/H_2-mesoporphyrin IX upon irradiation (Fig. 9a) is higher than that recorded in the dark (Fig. 9b). And the current is much higher than that recorded in the absence of H_2-mesoporphyrin IX (FTO/TiO_2, Fig. 9c). Therefore, the photoanode FTO/TiO_2/H_2-mesoporphyrin IX is photoelectrochemically active in the solution. This observation is consistent with the fact that the photoexcitation of the H_2-mesoporphyrin IX results in the generation of an electron.

Appropriate redesign of the PEBFC with more excellent performance is possible. For example, the improved photovoltaic performance may be obtained by co-sensitizing the porphyrin with other sensitizer on TiO_2 film electrode to enhance the light-harvesting capability of the PEBFC. And the enhanced

Table 2
Performances of the PEBFCs with H_2-mesoporphyrin IX or Zn-mesoporphyrin IX as sensitizer.

Dye	V_{oc} (mV)	I_{sc} (μA)	FF	P_{max} (μW cm^{-2})	η (%)
H_2-mesoporphyrin IX	767	90	0.46	139	0.14
Zn-mesoporphyrin IX	713	7	0.99	22	0.022

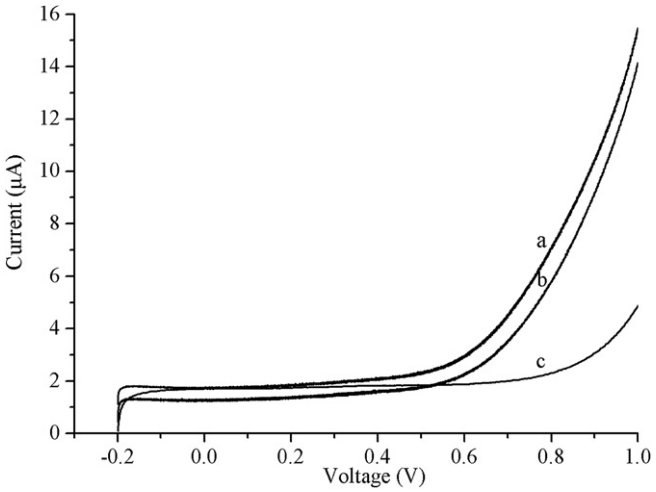

Fig. 9. Current–voltage curves of FTO/TiO_2/H_2-mesoporphyrin IX upon irradiation (a) or in the dark (b) and FTO/TiO_2 upon irradiation (c).

photovoltaic performance may be achieved by preparing highly ordered TiO_2 nanotube arrays to increase dye loading. And further work on optimizing the device performance is under way.

4. Conclusions

H_2-mesoporphyrin IX and Zn-mesoporphyrin IX with two carboxyl groups were successfully used as sensitizers to construct photoanodes of new two-compartment PEBFCs. The two PEBFCs can produce higher IPCEs than the reported PEBFCs based on porphyrin sensitizer with one carboxyl anchoring group. The UV–Vis and XPS spectra have confirmed that there are interactions between the sensitizer and TiO_2 film electrode, and their strengths are quite different and decreased in the order H_2-mesoporphyrin IX > Zn-mesoporphyrin IX. The FTIR data suggest that the two sensitizers are adsorbed via the bridging or the bidentate chelate coordination to the TiO_2 surface. Comparing the photovoltaic performance of the two PEBFCs based on the two sensitizers on TiO_2 film electrode, spectral difference was observed. The difference is due to the enhancement of the back electron-transfer process for the Zn-mesoporphyrin IX sensitizer. This result indicates that the structure of the sensitizer, that is, not only the existence of the metal but also the number of carboxyl anchoring group, is an important factor that must be considered when a PEBFC is constructed.

Acknowledgments

This work were supported by the National Basic Research Program of China (973 Program 2011CB935702) and the Foundation of Department of Education of Jilin Province of China (No. 2012400).

References

[1] L. de laGarza, G. Jeong, P.A. Liddell, T. Sotomura, T.A. Moore, A.L. Moore, D. Gust, J. Phys. Chem. B 107 (2003) 10252–10260.
[2] A. Brune, G. Jeong, P.A. Liddell, T. Sotomura, T.A. Moore, A.L. Moore, D. Gust, Langmuir 20 (2004) 8366–8371.
[3] M. Hambourger, A. Brune, D. Gust, A.L. Moore, T.A. Moore, Photochem. Photobiol. 81 (2005) 1015–1020.
[4] M. Hambourger, P.A. Liddell, D. Gust, A.L. Moore, T.A. Moore, Photochem. Photobiol. Sci. 6 (2007) 431–437.
[5] M. Hambourger, M. Gervaldo, D. Svedruzic, P.W. King, D. Gust, M. Ghirardi, A.L. Moore, T.A. Moore, J. Am. Chem. Soc. 130 (2008) 2015–2022.
[6] M. Hambourger, G. Kodis, M.D. Vaughn, G.F. Moore, D. Gust, A.L. Moore, T.A. Moore, Dalton Trans. (2009) 9979–9989.
[7] A. Yutaka, T. Yumi, Int. J. Hydrogen Energy 33 (2008) 2845–2849.
[8] A. Yutaka, T. Yumi, Int. J. Glob. Energy 28 (2007) 295–303.
[9] Q. Wang, W.M. Campbell, E.E. Bonfantani, K.W. Jolley, D.L. Officer, P.J. Walsh, K. Gordon, R. Humphry-Baker, M.K. Nazeeruddin, M. Grätzel, J. Phys. Chem. B 109 (2005) 15397–15409.
[10] A. Yella, H.W. Lee, H.N. Tsao, C.Y. Yi, A.K. Chandiran, M.K. Nazeeruddin, E.W.G. Diau, C.Y. Yeh, S.M. Zakeeruddin, M. Grätzel, Science 334 (2011) 629–634.
[11] M.P. Balanay, D.H. Kim, J. Mol. Struct. Theochem. 910 (2009) 20–26.
[12] W.M. Campbell, A.K. Burrell, D.L. Officer, K.W. Jolley, Coordination Chem. Rev. 248 (2004) 1363–1379.
[13] M.P. Balanaya, C.V.P. Dipalinga, S.H. Lee, D.H. Kima, K.H. Lee, Sol. Energy Mater. Sol. Cells 91 (2007) 1775–1781.
[14] M.P. Balanay, D.H. Kim, Curr. Appl. Phys. 11 (2011) 109–116.
[15] K.Q. Wang, J. Yang, L.G. Feng, Y.W. Zhang, L. Liang, W. Xing, C.P. Liu, Biosens. Bioelectron. 32 (2012) 177–182.
[16] P. Wang, S.M. Zakeeruddin, P. Comte, R. Charvet, R. Humphry-Baker, M. Grätzel, J. Phys. Chem. B 107 (2003) 14336–14341.
[17] J.A. Mikroyannidis, G. Charalambidis, A.G. Coutsolelosb, P. Balraju, G.D. Sharma, J. Power Sourc 196 (2011) 6622–6628.
[18] M.J. Lee, K.D. Seo, H.M. Song, M.S. Kang, Y.K. Eom, H.S. Kang, H.K. Kim, Tetrahedron Lett. 52 (2011) 3879–3882.
[19] N. Xiang, W.P. Zhou, S.H. Jiang, L.J. Deng, Y.J. Liu, Z. Tan, B. Zhao, P. Shen, S.T. Tan, Sol. Energy Mater. Sol. Cells 95 (2011) 1174–1181.
[20] Y. Tachibana, S.A. Haque, I.P. Mercer, J.R. Durrant, D.R. Klug, J. Phys. Chem. B 104 (2000) 1198–1205.
[21] A. Kay, M. Grätzel, J. Phys. Chem. 97 (1993) 6272–6277.
[22] T.L. Ma, K. Inoue, K. Yao, H. Noma, T. Shuji, E. Abe, J.H. Yu, X.S. Wang, B.W. Zhang, J. Electroanalytical. Chem. 537 (2002) 31–38.
[23] D. Shi, Y.M. Cao, N. Pootrakulchote, Z.H. Yi, M.F. Xu, S.M. Zakeeruddin, M. Grätzel, P. Wang, J. Phys. Chem. C 112 (2008) 17478–17485.
[24] V. Shklover, Y.E. Ovchinnikov, L.S. Braginsky, S.M. Zakeeruddin, M. Grätzel, Chem. Mater. 10 (1998) 2533–2541.
[25] D.M. Chen, D. Yang, J.Q. Geng, J.H. Zhu, Z.Y. Jiang, Appl. Surf. Sci. 255 (2008) 2879–2884.
[26] H. Spanggaard, F.C. Krebs, Sol. Energy Mater. Sol. Cells 83 (2004) 125–146.
[27] J. Yin, L. Qi, H.Y. Wang, Appl. Mater. Interfaces 3 (2011) 4315–4322.
[28] K. Takechi, T. Shiga, T. Motohiro, T. Akiyama, S. Yamada, H. Nakayama, K. Kohama, Sol. Energy Mater. Sol. Cells 90 (2006) 1322–1330.
[29] J. Yang, K.Q. Wang, L. Liang, L.G. Feng, B. Sun, W. Xing, Catal. Commun. 20 (2012) 76–79.
[30] T. Ma, K. Inoue, H. Noma, K. Yao, E. Abe, J. Photochem. Photobiol. A Chem. 152 (2002) 207–212.
[31] R.B.M. Koehorst, G.K. Boschloo, T.J. Savenije, A. Goossens, T.J. Schaafsma, J. Phys. Chem. B 104 (2000) 2371–2377.
[32] S. Cherian, C.C. Wamser, J. Phys. Chem. B 104 (2000) 3624–3629.
[33] S.A. Haque, Y. Tachibana, R.L. Willis, J.E. Moser, M. Grätzel, D.R. Klug, J.R. Durrant, J. Phys. Chem. B 104 (2000) 538–547.
[34] I. Bedja, S. Hotchandani, R. Carpentier, J. Appl. Phys. 75 (1994) 5444–5446.
[35] P.V. Kamat, I. Bedja, S. Hotchandani, L.K. Patterson, J. Phys. Chem. 100 (1996) 4900–4908.
[36] C. Nasr, P.V. Kamat, S. Hotchandani, Phys. Chem. B 102 (1998) 10047–10056.
[37] F. Fungo, L. Otero, E.N. Durantini, J.J. Silber, L.E. Sereno, J. Phys. Chem. B 104 (2000) 7644–7651.